TOPOLOGY OPTIMIZATION FOR 3D-PRINTABLE LARGE-SCALE METALLIC HOLLOW STRUCTURES WITH SELF-SUPPORTING

QIANG CUI[1], HUIKAI ZHANG[2], SIDDHARTH SUHAS PAWAR[3], CHUAN YU[4], XIQIAO FENG[5] and SONG QIU[6]

[1,6]*Academy of Arts and Design, Tsinghua University.*
[2,5]*Department of Engineering Mechanics, Tsinghua University.*
[3,4]*PIX Moving Inc.*
[1]*cui-q18@mails.tsinghua.edu.cn, 0000-0002-0876-5054*
[2]*zhk19@mails.tsinghua.edu.cn, 0000-0003-4792-6356*
[3]*smsusi@pixmoving.com, 0000-0002-6917-9489*
[4]*angelo@pixmoving.com, 0000-0001-6269-064X*
[5]*fengxq@tsinghua.edu.cn, 0000-0001-6894-7979*
[6]*qiusong@mail.tsinghua.edu.cn, 0000-0002-5230-1011*

Abstract. Design for Additive Manufacturing (DfAM), is a one of the most commonly used and foundational techniques used in the development of new products, and particularly those that involve large-scale metallic structures composed of hollow components. One such AM technique is Wire Arc Additive Manufacturing (WAAM), which is the application of robotic welding technology applied to Additive Manufacturing. Due to the lack of a simple method to describe the fabricating constraint of WAAM and the complex hollow morphology, which difficultly deploys topology optimization structural techniques that use WAAM. In this paper, we develop a design strategy that unifies ground-structure optimization method with generative design that considers the features of hollow components, WAAM overhang angle limits and manufacturing thickness limits. The method is unique in that the user can interact with the design results, make changes to parameters, and alter the design based on the user's aesthetic or specific manufacturing setup needs. We deploy the method in the design and 3D printing of an optimized Electric Vehicle Chassis and successfully test in under different loading conditions.

Keywords. Topology Optimization; Generative Design; Self-supporting; Hollow Structures; Metallic 3D Printing; SDG 12.

1. Introduction

Additive manufacturing technology has greatly been used in the fields of architecture, material science, vehicle and aircraft. It is a great challenge to manufacture low cost, short design cycle, strong reliability and integrated large-scale metallic structures. First of all, low cost requires us to use as few materials as possible to meet the design requirements. Many structures in nature have hollow tubular structures, which can not

POST-CARBON, Proceedings of the 27th International Conference of the Association for Computer-Aided Architectural Design Research in Asia (CAADRIA) 2022, Volume 2, 101-110.

only meet the nutrient transfer requirements of plants and animals with small materials but also maintain the stiffness and strength of tissues to a certain extent. Therefore, it is favored in the design of some energy-absorbing materials and large truss structures.

Secondly, the short design cycle requires an automated design process to select different tubular structures for optimization and integration. Therefore, the two problems to be faced here are that what kind of automatic topology optimization method should choose and how to describe tubular geometry. In terms of optimization methods, there are many topology optimization methods to find material distribution, including continuum (Aage, et al., 2017) and discrete ground structure (He, et al., 2017) topology optimization method. It is very difficult to describe hollow tubular geometry in a continuum optimization model, especially for three-dimensional and complex structures. A transformation continuum optimization models named a moving morphable components model (MMC) (Guo et al., 2014) try to design hollow vehicle hollow frames (Bai, et al., 2020), but the results are not ideal. It is relatively easy to describe hollow tubular structures in a discrete optimization model. The geometry of hollow tubular structures can be expressed by a few simple parameters.

Moreover, metallic additive manufacturing technology can greatly shorten the manufacturing cycle, and compared with traditional manufacturing technology, it can print some more complex shapes and structures; However, different additive manufacturing technologies have some geometric printing constraints on the internal details of the printed structure (Liu et al., 2018; Zhu et al., 2021); Therefore, it is important to consider specific printing constraint in the topology optimization process. Most of the previous researchers tried to consider some printing constraints into mathematical language, and then use them as constraints of optimization methods, to restrict the optimized structure to meet the geometric constraints of printing methods. It is difficult to achieve this goal in a continuum optimization model, especially in a three-dimensional complex model. Although some optimized structures can meet certain angle and size constraints in the ground topology optimization, they cannot satisfy the industrial aesthetics.

To sum up, motivation, the author of this paper, based on the traditional ground structure topology optimization framework, develop a new design method named generation design strategy, this method not only can satisfy WAAM (Xia et al., 2020) manufacturing constraints of a large-scale metallic hollow structure but at the same time also allows engineers to locally modify the structure of fast post-processing; Outdoor experiments verify that our designed products are high in structural safety and structural reliability.

2. Chassis of electric vehicle and load analysis

The design of the electric vehicle chassis (Figure 1a) is based on PIXBOT, a fully electric, four-hub motor drive, a four-wheel steered vehicle that is used as a platform for autonomous vehicles development by many companies and universities. Defining the design domain (Figure 1c) is the first step in our workflow. As shown in Figure 1c, the design domain geometry is constructed according to the shape of the original chassis and the layout of necessary components installed on the chassis (Figure 1b). To leave the maximum freedom to the optimization algorithm in search of the most optimal structure, the domain is made as large as possible. The battery pack, controller

and steering parts are defined as obstacle areas, while the other parts, such as holes for the electrical wires that supply power to the hub-motors, and holes for the steering rods, are defined as preserved areas. In addition, the wheelbase and the track of the vehicle are fixed. According to the actual size of the chassis, the design domain of the chassis is 2500mm in length, 1400mm in width and 400mm in height.

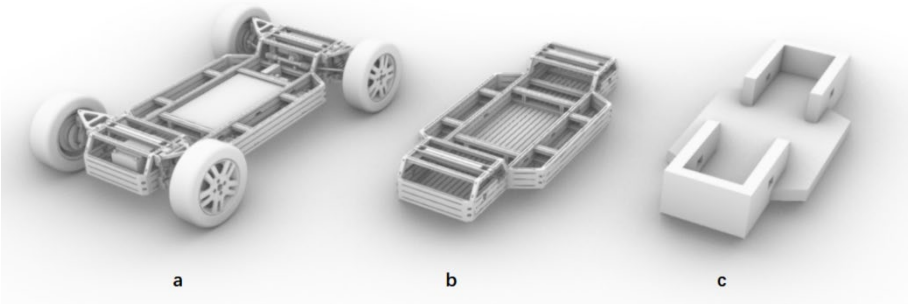

Figure 1. (a) The chassis with components; (b) The basic chassis structure; (c) Design domain of the chassis

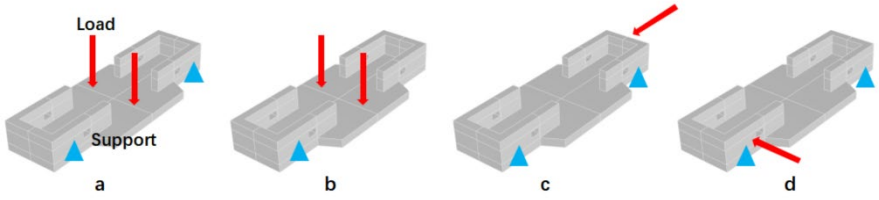

Figure 2. (a) Landing on four wheels; (b) Landing on three wheels; (c) Acceleration or deceleration; (d) Turning

The static load of the chassis is mainly composed of the weight of the chassis, the weight of the components and the weight of the cargo. The typical conditions should be analysed because of the complicated terrain encountered in the process of electric vehicle driving. There are four main types of load cases. The main working condition of an electric vehicle is landing on four wheels (Figure 2a). Under the condition of applying full load, the electric vehicle can land on four wheels and travel at a constant speed in good road conditions. The main load of the chassis includes its self-weight, weight of chassis components and cargo weight. In this case, the chassis is subjected to a vertical load and bending load. For landing on three wheels or the suspension system load (Figure 2b), one of the wheels of an electric car may leave the ground during rough roads. In this case, the chassis structure is subjected to severe torsional load. When the electric vehicle accelerates or decelerates (Figure 2c), the inertial force exerts a longitudinal load on the chassis structure. Its magnitude can be determined by the acceleration and the overall mass of the electric vehicle. When an electric vehicle turns (Figure 2d), the chassis structure tilts to one side under centrifugal force. The force is determined by the turning radius and driving speed.

When building a complex optimization model, secondary factors should be

ignored, which makes it easier to solve the model. There are many components of the chassis, and some components with a small load are omitted to reduce the number of stress points, such as computers, transformers, etc. In addition, because the structure of the frame is symmetric with the force, we only calculate a quarter of the model to speed up the calculation.

During the analysis, the weight of the chassis is applied by attaching a vertical downward gravitational acceleration. A load of each component is simply distributed to the stress point of the corresponding structure. For example, the total weight of the cargo 800kg is applied to the points at which the cargo rack is connected to the chassis. So, the points need to support at least 8000N of force downward (Figure 2). The influence of dynamic load on the chassis of the electric vehicle is considered by introducing a dynamic load factor and applying the load times to the dynamic load factor to the corresponding position during the finite element analysis of the chassis. According to the actual test, the dynamic load coefficient is selected to be 1.5.

3. Topology optimization and fabrication constraint

Topology optimization provides an efficient inverse analysis tool to design engineering structures with specific mechanical or other functions by using a minimal volume (or mass) of materials. For the continuous topology optimization method, the designed domain is discretized into many continuous and finite meshes. Various optimization methods, such as the solid interpolation of material penalty (SIMP) model (Aage et al., 2017), the level set model (Wang et al. 2003), and a moving morphable components model (MMC) (Guo et al., 2014), use a different framework to describe the design variables.

3.1. HOLLOW TUBULAR STRUCTURE

It is difficult for the continuous topology optimization method, such as the SIMP model and level-set method, to design the tubular structures (Clausen et al., 2015). In this method, the boundary of the tubes needs to be described by the complex mathematical formula, and they are not easily performed in large-scale structures and commercial software. Recently, the feature-driven MMC method (Bai et al., 2020) has been used to design the hollow tube framework of the vehicle, but the optimized results are too complex, and loose the aesthetics of the industrial products.

A discrete topology optimization method starts with a ground-structure model and produces optimized truss-like structures. For the stiffness problem, the optimization formula is written as (He et al, 2017; Ye et al., 2021; Zhang et al., 2017)

$$\min_{\mathbf{r}:} V = 2\pi \mathrm{t}\mathbf{I}^{\mathrm{T}}\mathbf{r}$$

$$\text{subject to: } \mathbf{Bq} = \mathbf{f},$$

$$-2\pi t\sigma_0 r_i \le q_i \le 2\pi t\sigma_0 r_i,$$

$$(0 \le r_i \le r^*), \quad i = 1,2,\dots,N,$$

where V is the structural volume, $\mathbf{I} = [l_1, l_2, \dots, l_{\mathrm{N}}]^{\mathrm{T}}$ is a vector of hollow tube length, N is the number of the hollow tube. We assume that all hollow tubes have a uniform wall thickness with $t = 2\mathrm{mm}$, $\mathbf{r} = [r_{1,} r_2 \dots, r_N]^{\mathrm{T}}$ is the vector of all hollow

tube radii and design variable, **f** and **q** are the vectors of the external nodal loads and internal force of hollow tube, respectively. The area of i-th hollow tube is approximate $a_i = 2\pi t r_i$. σ_0 =350.7MPa is the limiting tensile strength for the additive manufacturing material 7075 aluminum alloy. This discrete optimization process has three steps. In this model, the tube is easy to present by small geometrical parameters.

First, the design domain, load and supporting conditions are specified (Figure 3a). Next, the discrete nodes are generated inside the design domain and all possible members are created by interconnecting these nodes, forming a ground structure (Figure 3b). Then the problem can be solved by the optimization algorithm (e. g. the convex optimization) and the design variables are also be updated through mathematical iterations (Figure 3c). Finally, the discrete structures are transformed into a continuum of organic forms (Figure 3d). While, owing to the constraints of overhang, the optimized results generally cannot be fabricated through WAAM.

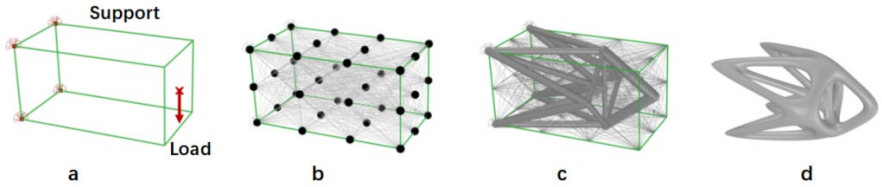

Figure 3: The schematic of the ground structure topology optimization. (a) Design domain; (b) Ground structure; (c) Optimization result; (d) Organic forms

3.2. FABRICATION CONSTRAINTS

Self-supporting 3D printing is a frontier fields for the manufacturing techniques and structural optimization. Recent attempts were made to study these geometric constraints in continuous topology optimization framework. However, these methods, containing complex mathematical descriptions of geometric constraints (Guo et al., 2017.) are too cumbersome for engineers and were found to not work well, especially for the design of large structures with complex loads. In addition, current topology optimization software cannot take manufacturing constraints into account at the design stage. For example, in our continuous topology optimization process, the optimized structure (Figure 4a) does not satisfy the manufacturing constraints of WAAM, as the resulting structures have sharp overhangs and the feature thickness at some locations is too low. To make the optimized results be manufacturable for the WAAM, manual and auto modification of these results were carried out as shown in Figure 4b-c, and the final results were still not promising.

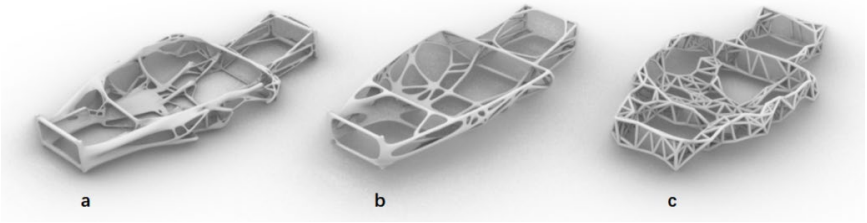

Figure 4: (a) Continuous topology optimization; (b) Manual modelling; (c) Auto modelling

3.3. GENERATIVE STRATEGY

Our initiative strategy to overcome this problem is to generate many possible results under one kind of load and boundary condition. There are three parameters in the topology optimization framework which we choose to vary:

M ∈{3, 5, 7, 9, 11}: where M is the number of the discretizing parts on each edge of the design domain, and M = 3 denotes that the three-dimensional design domain is divided with 3 × 3 × 3 nodes.

J∈{0, 0.1, 0.2, 0.5, 1}: The length of the i-th member is modified as $l_i + 2J$, J is the nodal penalizing factor that is used to reduce the number of short members in the optimized structures (Parker et al., 1975). The larger the value, the fewer the short members in the structure.

R ∈{0,1,2,5,10}: $R_i = \max(r_{i,j}), j = 1,2,..,n_i$, is the nodal merging radius of i-th node, and $r_{i,j} = ((\sum_{k=1}^{n_i}(1 + l_{i,j}.l_{i,k})a_{i,k})/(2\pi))^{1/2}$ (He et al., 2019).

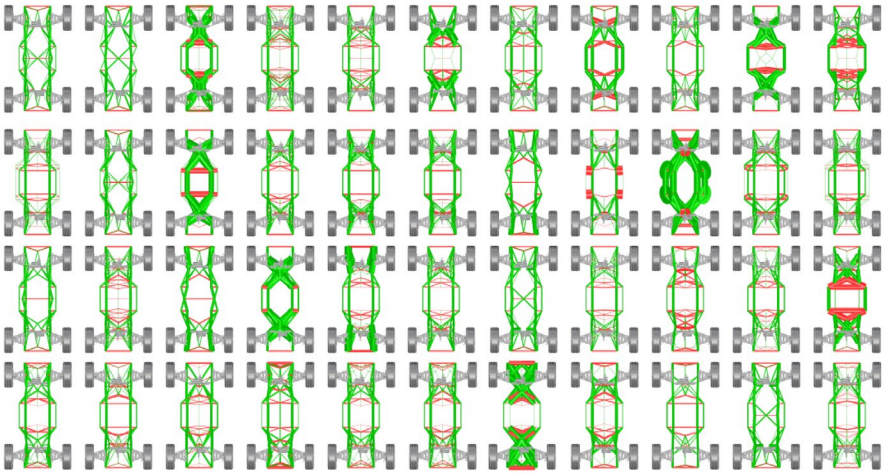

Figure 5. Part of the generated results. (Components greater than 60 degrees are marked in red)

By default, combining these factors leads to 1200 total chassis designs. Figure 5 represents part of the generated results, where green parts can be WAAM printed while red parts cannot be. Each design takes an average of 2 seconds to calculate, requiring 40 minutes total. In order to get manufacturable and lightweight solutions, our generated results also should satisfy the following expectations:

minize: $\{V_{\min}^{(j)} \mid j\epsilon\Omega\}$, and $\{n_j | j\epsilon\Omega,$ in which $\theta_i \leq 60^0, i\epsilon N\}$,

where Ω is the sets of generated results, $V_{\min}^{(j)}$ is the minimum material volume of the j-th result in Ω; n_j is the number of tubes in the j-th generated structure with an inclination θ_i to the horizontal plane.

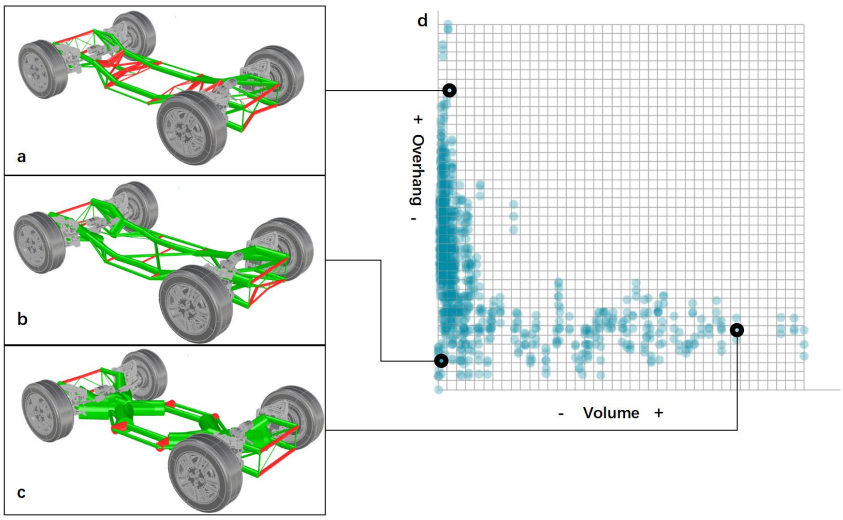

Figure 6. Objective space

We chose the final solution in an interactive way rather than an automatic optimization. In order to clearly understand the attributes of all solutions, we can visualize the results by plotting a Pareto front of the two objective function values. Figure 6d shows each chassis design as a point on a scatter plot where the x-axis represents the weight of the chassis, the y-axis represents the number of overhang hollow components. The performance values of each design are mapped to the coordinate system. Fig 6a shows one of the obtained design results of a lightweight chassis with a large number of overhang hollow components. Fig 6b shows a lightweight chassis with a low number of overhang hollow components, therefore having much greater manufacturability. Fig 6c shows a very heavy chassis with a large number of overhang hollow components.

Once the result is determined, the user has a further choice to locally edit the final results to meet the aesthetic and manufacturing constraint of WAAM, without fundamentally altering the design. For instance, the user can go into the edit mode, click on the element that needs to be changed and rebuild its size or change the position of the joint nodes. Manual modification is useful when the structural complexity of obtained results is relatively low. It has a high dependency on the artistic skill of the designer or engineer and cannot be scaled to highly complex structures.

To get a continuous, smooth and organic structure, we apply the SubD algorithm to our optimized result (Figure 7a). In Rhino7.0, MultiPipe can make a smooth piped surface out of a network of curves with a smooth joint at each curve intersection, at the same time adhering to the optimized cross-sectional area values obtained after optimization. In Figure 7b, the optimized hollow structure can be directly imported in the commercial finite element software Abaqus. The 7075 aluminum alloy with its material density, Youg's modulus and Poisson's ratio $2810\ kg/m^3$, 71 GPa and 0.33, is taken in our simulations and the printed structures, and the von-Mises stress and

lower-frequency modes of the optimized hollow structures are calculated using shell model in the software Abaqus, and the results (Figure 7c) show that the optimized structures have great strength and reliability.

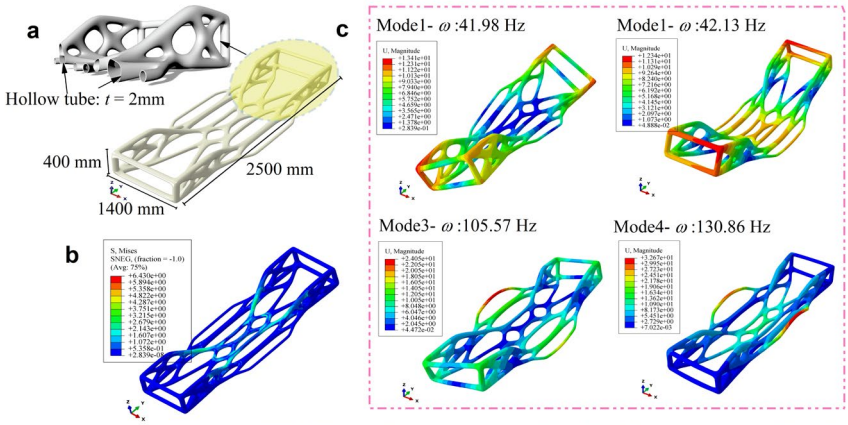

Figure 7: (a) Smoothed hollow structure; (b) von-Mises stress of the optimized structure; (c) Modal analysis

4. Fabrication

WAAM is an emerging AM technology that uses a combination of an electric arc as a heat source and a metal wire as feedstock. The hardware included a KUKA six-axis robot, a Fronius CMT welding equipment. No part-rotator was used.

A key factor that allows the model to be manufactured is path planning. The model is sliced into horizontal layers and each layer is further broken down into a list of points with their respective orientation for the robot to reach. The orientation of each point is defined by a unit normal vector that is normal to the surface of the optimized final result geometry at that point. This is the orientation the robotic end-effector will be aligned in the 3D printed object and is critical because it allows the weld bead to have a maximum area of contact with the weld pool. The method is different from the traditional desktop 3D printing process wherein the printing head is always aligned vertically, thereby reducing its ability to print at sharp overhang angles without a support structure.

The final designed chassis has a dimension of 2500 mm × 1400 mm × 400 mm, made from high specific strength aluminium alloy 7075, was printed in 80 hours, and weighs about 60kg (Figure 8). The 3D printing chassis is half as heavy as the previous chassis (PIXBOT). The cost of aluminium filament wire used for 3D printing is about 10 US dollars/kg, and for the final designed 60kg chassis, this amounts to a cost of 600 dollars. If we do not consider the initial investments made in acquiring the robot and the welding equipment, the only other cost is that of electricity.

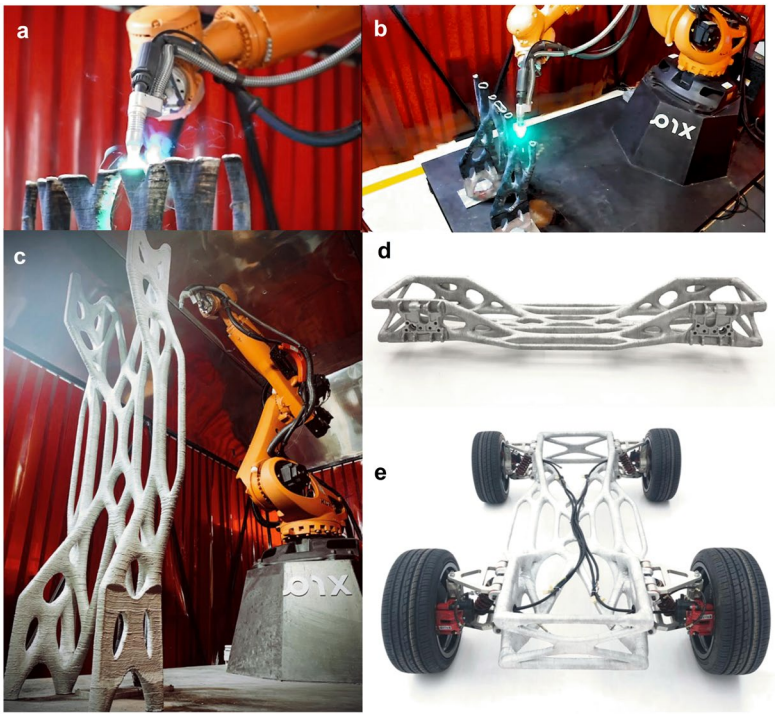

Figure 8: (a), (b) and (c) Manufacturing process; (d) Chassis printing part; (e) Chassis assembly

5. Discussion

Our work contributes to the development of a method that allows user to fabricate large-scale structurally optimized results for a given load-case while considering WAAM manufacturability simultaneously. To the best of the authors' knowledge, no computational tools currently exist that perform structural optimization design while considering WAAM manufacturing constraints and our work addresses this problem. We first justify the use of WAAM as an extremely economical and production-scalable AM technique due to it's low running costs and high metal deposition rates. We then address the problem through a unification of truss-network based continuous layout optimization, hollow model of tube, aesthetics and further manufacturing consideration of the user through user-interaction with the model, creation of a final organic shape with a smooth transition of the hollow tube network at the joints. The method is used to design and fabricate the world's first metal 3D-printed full-scale Electric-Vehicle chassis that has been successfully tested for strength and durability in real-road conditions.

References

Aage, N., Andreassen, E., Lazarov B. S., & Sigmund, O. (2017). Giga-voxel computational morphogenesis for structural design.

Nature, 550, 84-86.
https://doi.org/10.1038/nature23911

Bai, J. T., & Zuo, W. J. (2020). Hollow structural design in topology optimization via moving morphable component method.
Structural and Multidisciplinary Optimization, 6, 187-205.
https://doi.org/10.1007/s00158-019-02353-0

Clausen, A., Aage, N.., Sigmund, O. (2015). Topology optimization of coated structures and material interface problems.
Computer Methods in Applied Mechanics and Engineering, 290, 524-541.
https://doi.org/10.1016/j.cma.2015.02.011.

Guo, X., Zhou, J. H., Zhang, W. S., Du, Z. L., Liu, C., Liu, Y. (2017). Self-supporting structure design in additive manufacturing through explicit topology optimization.
Computer Methods in Applied Mechanics and Engineering, 323, 27-63.
https://doi.org/10.1016/j.cma.2017.05.003

Guo, X., Zhang, W. S., & Zhong, W. L. (2014). Doing topology optimization explicitly and geometrically-a new moving morphable components based framework.
Journal of Applied Mechanics, 81, 081009.
https://doi.org/10.1115/1.4027609

He, L. W., Matthew, G., & Song, X. Y. (2019). A python script for adaptive layout optimization of trusses.
Structural and Multidisciplinary Optimization, 60, 835-847.
https://doi.org/10.1007/s00158-019-02226-6

Liu, J. K., Gaynor A. T., Chen, S. k., Kang, Z., Suresh, K., Takezawa, A., Li, L., Kato, J. J, Tang, J. Y., Wang, Charlie C. L., Cheng, L., Liang, X., & To, A. C. (2018). Current and future trends in topology optimization for additive manufacturing.
Structural and Multidisciplinary Optimization, 57, 2457–2483.
https://doi.org/10.1007/s00158-018-1994-3

Parkes, E. W. (1975) Joints in optimization frameworks.
International Journal of Solids and Structures, 11, 1017-1022.

Wang, M. Y., Wang, X. M., Guo, D. M. (2003). A level set method for structural topology optimization.
Computer Methods in Applied Mechanics and Engineering, 192, 227-246.

Xia, C. Y., Pan, Z. X., Polden, J., Li, H. J., Xu, Y. L., Chen, S. B., Zhang, Y. M. (2020). A review on wire arc additive manufacturing: Monitoring, control and a framework of automated system.
Journal of Manufacturing Systems, 57, 31-45.
https://doi.org/10.1016/j.jmsy.2020.08.008

Ye, J., Kyvelou, P., Gilardi, F., Lu, H. J., Gilbert, M., & Gardner L. (2021) An end-to-end framework for the additive manufacture of optimized tubular structures. *IEEE Access.*
https://doi: 10.1109/access.2021.3132797

Zhang, X. J., Ramos, A. S., Paulino, G. H. (2017). Material nonlinear topology optimization using the ground structure method with a discrete filtering scheme.
Structural and Multidisciplinary, 55, 2045–2072.

Zhu, J. H., Zhou, H., Wang, C., Zhou, L., Yuan, S. Q., Zhang, W. H. (2021) A review of topology optimization for additive manufacturing: Status and challenges.
Chinese Journal of Aeronautics, 34, 91-110.
https://doi.org/10.1016/j.cja.2020.09.020